Journal of Medicinal Chemistry

Article

pubs.acs.org/jmc

Synthesis and Evaluation of ^{18}F-Labeled Styryltriazole and Resveratrol Derivatives for β-Amyloid Plaque Imaging

Iljung Lee, Yearn Seong Choe,* Joon Young Choi, Kyung-Han Lee, and Byung-Tae Kim

Department of Nuclear Medicine, Samsung Medical Center, Sungkyunkwan University School of Medicine, 50 Ilwon-dong, Kangnam-ku, Seoul 135-710, Korea

Supporting Information

ABSTRACT: In the present study, a styryltriazole and four resveratrol derivatives were synthesized as candidates for β-amyloid (Aβ) plaque imaging. On the basis of their binding affinities to Aβ(1−42) aggregates, the styryltriazole (**1**, K_i = 12.8 nM) and one resveratrol derivative (**5**, K_i = 0.49 nM) were labeled with ^{18}F. In normal mice, tissue distribution of [^{18}F]**5** showed good initial brain uptake (3.26% ID/g at 2 min) but slow wash-out from brains (2-to-60 min uptake ratio: 2.9). Furthermore, it underwent in vivo metabolic defluorination (1.88% ID/g at 2 min and 9.73% ID/g at 60 min). In contrast, [^{18}F]**1** displayed high initial brain uptake (5.38% ID/g at 2 min) with rapid wash-out from brains (0.52% ID/g at 60 min; 2-to-60 min uptake ratio: 10.3). These results indicate that [^{18}F]**1** has in vivo kinetics comparable to PET radiopharmaceuticals currently under commercial development, demonstrating that [^{18}F]**1** is a desirable PET radioligand for Aβ plaque imaging.

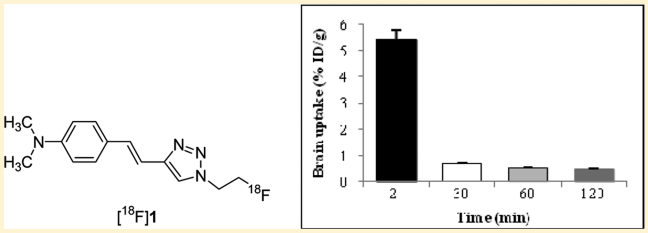

INTRODUCTION

Alzheimer's disease (AD) is characterized by the accumulation of Aβ plaques and neurofibrillary tangles (NFTs) in the brain, which may play a major role in development of the disease.[1−3] Therefore, in vivo imaging of Aβ plaques and NFTs may be beneficial for the diagnosis, staging, and treatment of AD.

Most Aβ plaque imaging radioligands have been developed based on highly conjugated fluorescent dyes.[4] A neutral and lipophilic fluorescent dye, 2-(1-{6-[dimethylamino]-2-naphthyl}ethylidene)malononitrile (DDNP) was developed as [^{18}F]FDDNP, which was shown to penetrate easily the blood−brain barrier (BBB) due to its high lipophilicity (log P = 3.92). This radioligand was found to label both Aβ plaques and NFTs in the brains of AD patients with PET.[5,6] Radiolabeled styrylbenzene derivatives were derived from Congo red and Chrysamine G, and radiolabeled benzothiazole derivatives were modified from thioflavin-T (Figure 1). It was also shown that there are two different binding sites on Aβ(1−40) and Aβ(1−42) aggregates under competitive binding assay conditions, which was confirmed with the use of ^{125}I-labeled styrylbenzenes and benzothiazoles.[7] A neutral benzothiazole derivative, [^{11}C]6-OH-BTA-1 ([^{11}C]PIB), has been the most well-characterized radioligand with minimal retention in the subcortical white matter of AD patients compared with other benzothiazole-based radioligands.[8−12] Another ^{11}C-labeled benzothiazole ligand, 2-(6-([^{11}C]methylamino)pyridin-3-yl)benzo[*d*]thiazol-6-ol ([^{11}C]AZD2184, K_i = 19.7 nM) may also be a promising Aβ plaque imaging agent because [^{3}H]AZD2184 showed a higher prefrontal cortex to subcortical white matter uptake ratio than [^{3}H]PIB in cortical brain sections from transgenic mice and from AD patients.[13] An imidazo[2,1-*b*]benzothiazole (IBT) derivative, 2-(*p*-methylaminophenyl)-7-methoxyimidazo[2,1-*b*]-benzothiazole, had high in vitro binding affinity to Aβ aggregates (K_i = 3.5−5.8 nM), and its ^{11}C-labeled ligand demonstrated high initial brain uptake (9.2% ID/g at 5 min postinjection) with fast wash-out (5-to-30 min ratio = 9.1) in normal Balb-C mice. MicroPET of transgenic APP/PS1 mouse brain and auto-radiography of transgenic mouse brain sections demonstrated that this radioligand binds to Aβ plaques.[14] Small (*E*)-stilbenes containing an electron-donating group showed high binding affinity to Aβ aggregates. (*E*)-4-Methylamino-4′-hydroxystil-bene ([^{11}C]SB-13) displayed good in vitro binding affinity to Aβ(1−40) aggregates (K_i = 6.0 nM) and showed high initial brain cortex uptake in normal rats (1.51% ID/g at 2 min) and rapid wash-out (0.42% ID/g at 30 min). This radioligand was also shown to label specifically Aβ plaques in brain sections from transgenic CRDN8 mice.[15] ^{125}I-Labeled radioligands have been also developed, including 2-[4′-(dimethylamino)-phenyl]-6-iodobenzothiazole (TZDM, K_i = 1.9 nM),[16] 2-(4′-dimethylaminophenyl)-6-iodobenzoxazole (IBOX, K_i = 0.8 nM),[17] and 6-iodo-2-(4′-dimethylamino-)phenyl-imidazo[1,2-*a*]-pyridine (IMPY, K_i = 15 nM).[18] Although [^{125}I]TZDM and [^{125}I]IBOX did label Aβ plaques in post-mortem AD brain sections, they showed slow wash-out from normal mouse brain.[16,17] Whereas [^{125}I]IMPY showed good initial brain uptake (2.88% ID/organ at 2 min) with rapid wash-out in normal mice and labeled regions containing Aβ plaques in transgenic PSAPP mouse brain sections, and in post-mortem

Received: October 18, 2011
Published: January 11, 2012

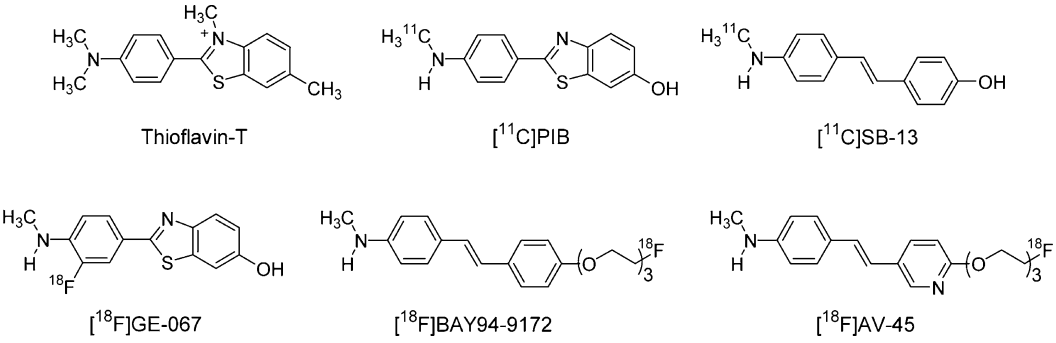

Figure 1. Chemical structures of thioflavin-T, [^{11}C]PIB, [^{11}C]SB-13, [^{18}F]GE067, [^{18}F]BAY94−9172, and [^{18}F]AV-45.

AD brain sections, [^{123}I]IMPY showed poor signal-to-noise ratio in human PET studies.[18−21]

Recently, ^{18}F-labeled ligands have been developed to overcome the limitation of the short half-life of ^{11}C. SB-13 was modified to give 1,2-diphenylacetylene, where the double bond was replaced by a triple bond and the hydroxyl group was fluoropegylated. These ligands showed high binding affinities to AD brain homogenates (K_i = 1.2−2.9 nM), and their ^{18}F-labeled ligands displayed desirable properties in normal mouse brains.[22] In addition, the double bond of SB-13 was replaced by a triazole moiety via click chemistry to synthesize 1,4-diphenyltriazole derivatives.[23] Click chemistry, which is a Cu(I)-catalyzed Huisgen 1,3-dipolar cycloaddition between terminal alkynes and azides, has been widely used to readily synthesize various triazoles in high yield.[24−26] 1,4-Diphenyltriazole derivatives (K_i = 4−30 nM to Aβ plaques in AD brain homogenates) were labeled with ^{18}F or ^{125}I, which had relatively good pharmacokinetics in normal mouse brains (2-to-30 min ratio = 2.31−5.66).[27] Recently, AZD4694 (2-(2-fluoro-6-(methylamino)pyridin-3-yl)benzofuran-5-ol) was developed, and it was found that [^{3}H]AZD4694 specifically labeled Aβ deposits in gray matter with a low level of white matter retention in the cortical sections from post-mortem AD brain.[28] A preclinical study of [^{18}F]AZD4694 in cynomolgus monkeys showed high uptake by the brain (5.2% ID at 1.5 min) with rapid wash-out (0.5% ID at 55 min), and the peak to 55 min ratio was twice as high compared with that of [^{11}C]PIB.[29] A recently developed 2-(*p*-methylaminophenyl)-7-(2-[^{18}F]-fluoroethoxy)imidazo[2,1-*b*]benzothiazole displayed high initial brain uptake (7.1% ID/g at 5 min postinjection) with fast wash-out (5-to-30 min ratio = 5.6) in normal Balb-C mice. This radioligand showed promise as an Aβ plaque imaging agent based on microPET of transgenic APP/PS1 mouse brain and autoradiography of transgenic mouse brain sections.[30]

Three ^{18}F-labeled ligands are currently under commercial development, including 2-(3-[^{18}F]fluoro-4-(methylamino)-phenyl)benzo[*d*]thiazol-6-ol (GE-067, K_i = 0.74 nM),[31,32] (*E*)-4-(2-(4-(2-(2-(2-[^{18}F]fluoroethoxy)ethoxy)ethoxy)phenyl) vinyl]-*N*-methylaniline (BAY94−9172, K_i = 2.22 nM),[33,34] and (*E*)-4-(2-(6-(2-(2-(2-[^{18}F]fluoroethoxy)ethoxy)ethoxy)pyridin-3-yl)vinyl)-*N*-methylaniline (AV-45, K_i = 2.87 nM)[35] (Figure 1). The preliminary results demonstrated that these ^{18}F-labeled ligands are potentially useful for PET imaging of Aβ plaques in AD patient brains.[31−36]

Resveratrol (trans-3,4′,5-trihydroxylstilbene), a grape-derived polyphenol, is known to have neuroprotective, cardioprotective, and cancer chemopreventive activity, and epidemiologic studies have shown that moderate wine intake reduces the risk of developing AD.[37−39] Specifically, resveratrol has been reported to promote the intracellular degradation of Aβ via a mechanism associated with the proteasome.[40] It was also shown that resveratrol inhibits Aβ42 fibril formation and cytotoxicity, but it does not prevent Aβ oligomer formation.[41] A ^{18}F-labeled resveratrol derivative, in which the 4′-OH was replaced by ^{18}F, displayed high radioactivity uptake in the liver and kidneys with subsequent hepatobiliary and renal excretion in normal Wistar rats, but it had low brain uptake (0.33% ID/g at 5 min and 0.05% ID/g at 60 min postinjection).[42]

In the present study, we designed fluorine-substituted resveratrol derivatives because of known neuroprotective activity of resveratrol and its structure similar to SB-13 (Figure 1) and also designed a styryltriazole, in which a phenyl ring of stilbene was replaced by a triazole. Selected ligands, **1** and **5**, were radiolabeled with ^{18}F and evaluated as PET radioligands for Aβ plaque imaging.

RESULTS AND DISCUSSION

Chemistry. The key step for styryltriazole and resveratrol derivative synthesis was the Wadsworth−Emmons reaction between the aldehyde and phosphonate carbanion. In this reaction, only the *E*-isomer is obtained because of steric hindrance on both aromatic groups. We confirmed that ligands **1**-**5** were *E*-isomers based on ^{1}H NMR analysis (J = 16.0−17.0 Hz, styrylvinyl protons).[43]

The synthetic pathway for the stryltriazole derivative **1** is shown in Schemes 1 and 2. The diethyl phosphonate fragment **6** was prepared from 4-nitrobenzyl bromide in high yield (85%). The aldehyde fragment **7** was synthesized in three steps; click chemistry between 2-azidoethanol and 3,3-diethoxy-1-propyne in the presence of $CuSO_4{\cdot}5H_2O$ and sodium ascorbate,[24] followed by reduction of diethyl acetal and then MOM protection of the OH group (Scheme 2). A color change from green to yellow was observed in the triazole-containing reaction solution and a singlet peak between 7.79 and 8.27 ppm on ^{1}H NMR analysis identified the triazole proton. Compound **8** was prepared in 65% yield from a Wadsworth−Emmons reaction between **6** and **7**. In this reaction, *t*-BuOK was added to the reaction mixture at 0 °C as the addition of *t*-BuOK at room temperature gave the product in a lower yield (<20%). Reduction of the nitro group in **8** under acidic conditions resulted in simultaneous deprotection of MOM group, which gave **9**. *N*,*N*-Dimethylation of the amine group in **9**, followed by methanesulfonylation of the OH group in **10**, gave the precursor **11**. Although a Wadsworth−Emmons reaction between dimethylaminobenzyl phosphonate and **7** was attempted, the reaction was not successful, most likely because it was difficult to produce the phosphonate carbanion due to the presence of an electron-donating group at the *para*-position. Nucleophilic

dx.doi.org/10.1021/jm201400q | J. Med. Chem. 2012, 55, 883−892

Scheme 1[a]

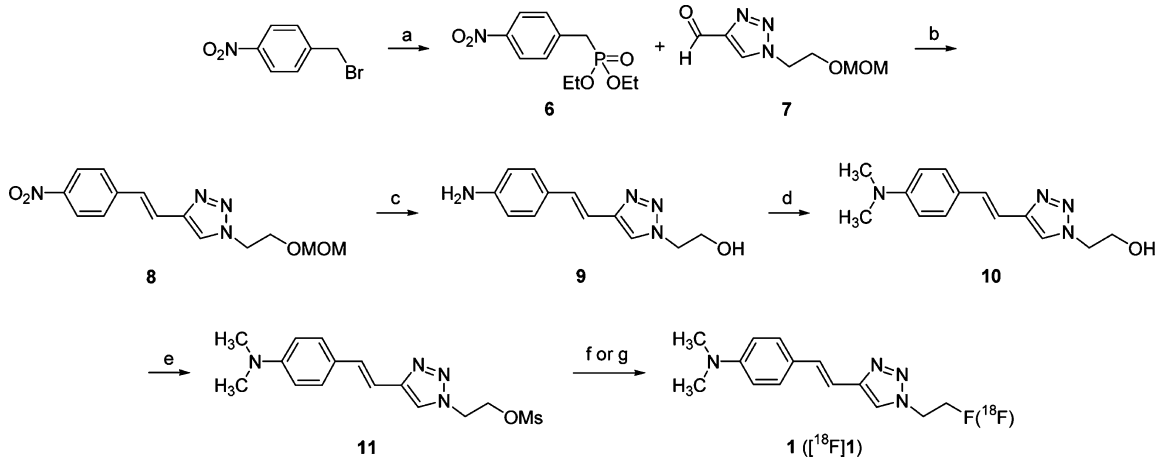

[a]Reagents and conditions: (a) $P(OEt)_3$, 160 °C, 3 h; (b) *t*-BuOK, DMF, room temperature, 1 h; (c) $SnCl_2{\cdot}2H_2O$, conc. HCl, EtOH, 80 °C, 2 h; (d) $(CHO)_n$, $NaBH_3CN$, acetic acid, room temperature, 20 h; (e) MsCl, Et_3N, CH_2Cl_2, room temperature, 2 h; (f) CsF, CH_3CN, 100 °C, 10 h; and (g) *n*-$Bu_4N[^{18}F]F$, CH_3CN, 90 °C, 10 min.

Scheme 2[a]

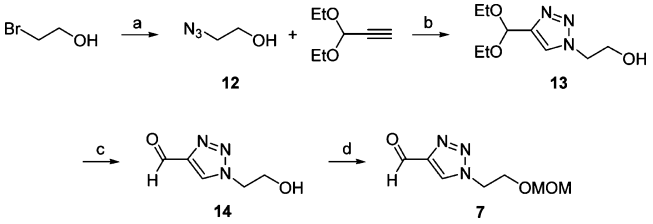

[a]Reagents and conditions: (a) NaN_3, water, 85 °C, 16 h; (b) sodium ascorbate, $CuSO_4{\cdot}5H_2O$, *t*-BuOH, water, room temperature, 4 h; (c) 50% TFA (aq), $CHCl_3$, 0 °C, 2 h; and (d) MOMCl, DIPEA, THF, 65 °C, 16 h.

fluorination of **11** with CsF gave styryltriazole **1**. In addition, fluorination of **10** with diethylaminosulfur trifluoride (DAST) was attempted;[44] however, this one-step reaction gave **1** in lower yield (19.8%) compared with a two-step reaction from **10** to **1** (33.4%) (Scheme 1).

The synthetic pathways for the resveratrol derivatives **2**–**5** are shown in Schemes 3–5. Ligands **2**, **4**, and **5** were prepared

Scheme 3.[a]

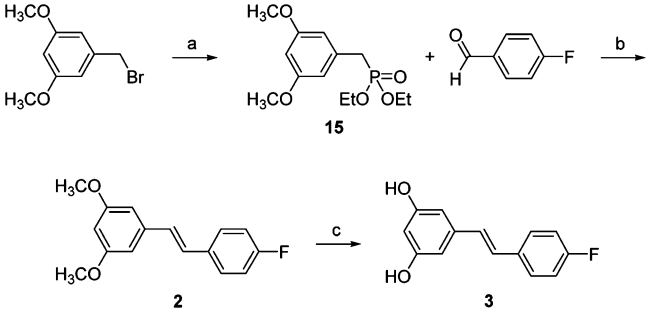

[a]Reagents and conditions: (a) $P(OEt)_3$, DMF, 160 °C, 4 h; (b) *t*-BuOK, DMF, room temperature, 1 h; and (c) BBr_3, CH_2Cl_2, room temperature, 20 h.

by the Wadsworth–Emmons reaction[45,46] between **15** as the phosphonate carbanion and the corresponding benzaldehyde derivatives (4-fluorobenzaldehyde, **16**, or **17**) in the presence of *t*-BuOK in DMF. Compound **15** was synthesized from 3,5-dimethoxybenzyl bromide and triethyl phosphite in high yield (99%). The fluoroalkyloxy benzaldehyde derivatives **16** and **17** were prepared from 4-hydroxybenzaldehyde and the corresponding fluoroalkyl tosylate in the presence of K_2CO_3 in CH_3CN in high yields (95%) (Scheme 4).[47] Ligand **3** was synthesized by *O*-demethylation at the 3,5-positions of the phenyl ring in **2** in 56% yield (Scheme 3).[48,49] The tosylate precursor **22** for [^{18}F]**5** synthesis was prepared from 4-hydroxybenzaldehyde in five steps (Scheme 5).

Radiochemical Synthesis of [^{18}F]1 and [^{18}F]5. [^{18}F]**1** was synthesized from **11** and *n*-$Bu_4N[^{18}F]F$ at 90 °C for 10 min (Scheme 1). The following HPLC purification gave [^{18}F]**1** in an overall 25–30% decay-corrected radiochemical yield and radiochemical purity higher than 99% with a specific activity of 37.6 GBq/μmol. The total synthesis time, including HPLC purification, was 60 min. We also considered radiochemical synthesis of [^{18}F]**1** using click chemistry; however, preparation of (*E*)-4-(but-1-en-3-ynyl)-*N*,*N*-dimethylaniline, a terminal alkyne for click chemistry, could not be possible. Furthermore, it would result in a two-step radiolabeling method. [^{18}F]**5** was synthesized from **22** and *n*-$Bu_4N[^{18}F]F$ at 110 °C for 10 min (Scheme 5). The following HPLC purification gave [^{18}F]**5** in an overall 56% decay-corrected radiochemical yield and radiochemical purity higher than 99% with a specific activity of 37.8 GBq/μmol. The total synthesis time, including HPLC purification, was 60 min.

In Vitro Binding Assays. In vitro binding assays were conducted using the same method as previously described.[16] The K_d value of [^{125}I]TZDM for binding to Aβ(1–42) aggregates was 0.37 nM, which is similar to the reported value of 0.14 nM.[16] The K_i value of TZDM was 2.01 nM, which is comparable to the reported value of 2.2 nM.[16] The K_i values of ligands **1**–**5** for Aβ(1–42) aggregates ranged from 0.49 to 39.7 nM (Table 1); of these ligands, the fluoroethyl (**4**) and fluoropropyl resveratrol derivatives (**5**) showed excellent binding affinities (K_i = 0.74 and 0.49 nM). The binding affinity of **3** (K_i = 39.7 nM) was significantly decreased by *O*-demethylation at the 3,5-positions of **2** (K_i = 4.91 nM). This result suggests that methoxy groups at the 3,5-positions are

dx.doi.org/10.1021/jm201400q | J. Med. Chem. 2012, 55, 883–892

Scheme 4[a]

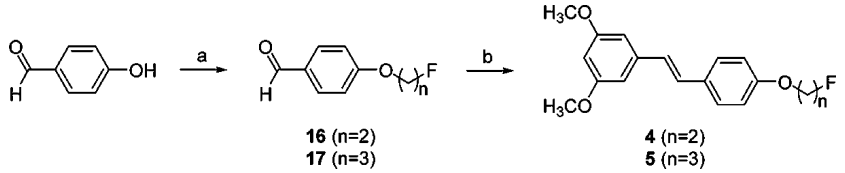

[a]Reagents and conditions: (a) fluoroalkyl tosylate, K_2CO_3, CH_3CN, 70 °C, 17 h; and (b) **15**, *t*-BuOK, DMF, room temperature, 1 h.

Scheme 5[a]

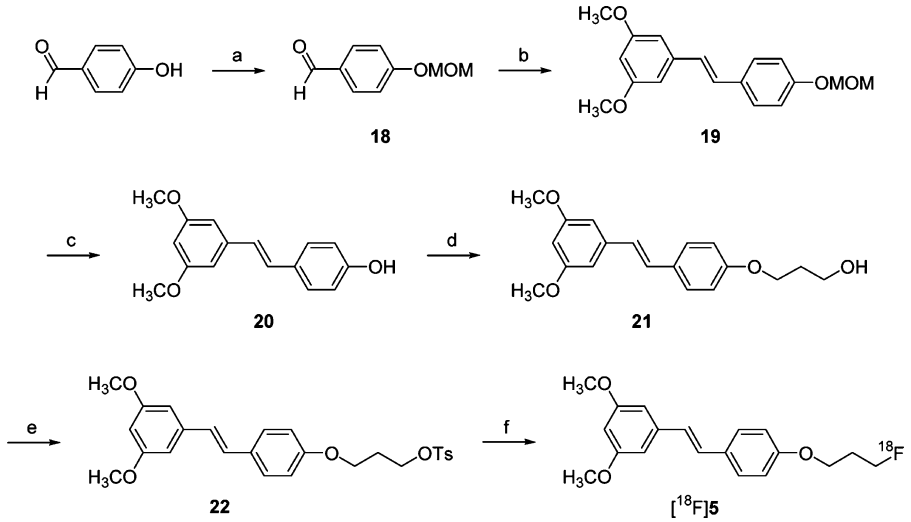

[a]Reagents and conditions: (a) MOMCl, DIPEA, THF, 65 °C, 20 h; (b) **15**, *t*-BuOK, DMF, room temperature, 1 h; (c) 6 N HCl, THF, room temperature, 1 h; (d) 3-chloropropanol, K_2CO_3, DMF, 160 °C, 20 h; (e) TsCl, Et_3N, CH_2Cl_2, room temperature, 2 h; and (f) *n*-$Bu_4N[^{18}F]F$, CH_3CN, 110 °C, 10 min.

Table 1. K_i (nM) of Ligands for Aβ(1-42) Aggregates

ligand	K_i (nM)
TZDM	2.01 ± 0.03
1	12.8 ± 0.77
2	4.95 ± 5.45
3	39.7 ± 17.02
4	0.74 ± 0.26
5	0.49 ± 0.15

Table 2. Tissue Distribution of [^{18}F]1 in Normal Mice[a]

organ	2 min	30 min	60 min	120 min
blood	3.35 ± 0.33	2.16 ± 0.14	1.27 ± 0.13	0.98 ± 0.13
heart	3.80 ± 0.11	1.32 ± 0.05	0.81 ± 0.04	0.71 ± 0.04
lung	5.73 ± 0.31	1.75 ± 0.08	1.04 ± 0.02	0.76 ± 0.04
liver	12.50 ± 1.28	7.59 ± 1.30	3.47 ± 0.92	3.47 ± 0.69
spleen	2.36 ± 0.67	0.85 ± 0.06	0.60 ± 0.04	0.49 ± 0.03
kidney	7.32 ± 2.37	7.32 ± 3.06	3.70 ± 1.64	1.86 ± 0.54
muscle	2.44 ± 0.83	0.74 ± 0.05	0.51 ± 0.02	0.40 ± 0.04
femur	1.49 ± 0.19	0.70 ± 0.04	0.94 ± 0.06	1.54 ± 0.02
brain	5.38 ± 0.38	0.68 ± 0.02	0.52 ± 0.02	0.48 ± 0.02

[a]Values (% ID/g) are given as the means ± SD of groups, n = 4 mice.

required for high binding affinity to Aβ(1−42) aggregates. In addition, it was reported that initial brain uptake of [^{18}F]**3** was low (0.33% ID/g at 5 min postinjection) in normal Wistar rats.[42] The styryltriazole derivative, **1**, displayed good binding affinity to Aβ(1−42) aggregates (K_i = 12.8 nM). Ligands **1** and **5** were selected for radiolabeling with ^{18}F because **5** had the highest binding affinity, and **1** contained a triazole moiety despite its lower binding affinity than most other resveratrol derivatives, **2**, **4**, and **5**.

Partition Coefficient Measurement of [^{18}F]1 and [^{18}F]5. The partition coefficients of **1** and **5** were measured using [^{18}F]**1** and [^{18}F]**5**, having log *P* values of 1.74 and 2.84, respectively. These values are suitable for favorable brain permeability.[36]

Tissue Distribution of [^{18}F]1 and [^{18}F]5 in Normal Mice. Tissue distribution of [^{18}F]**1** showed high radioactivity accumulation in the liver (12.50% ID/g) and in the kidneys (7.32% ID/g) at 2 min postinjection, which decreased over time (Table 2). Brain uptake of [^{18}F]**1** was 5.38% ID/g at 2 min, 0.68% ID/g at 30 min, and 0.52% ID/g at 60 min postinjection with high 2-to-30 min and 2-to-60 min uptake ratios of 7.9 and 10.3, respectively (Figure 2A), fulfilling desirable pharmacokinetics for Aβ plaque imaging radioligands. It should be noted that high initial brain uptake (>4% ID/g at 2 min postinjection) with fast wash-out kinetics in normal mice (<30% of initial uptake at 30 min) is required for Aβ plaque imaging radioligands.[22] [^{18}F]**1** did not appear to undergo metabolic defluorination due to a constant level of femur uptake over time (0.70 to 1.54% ID/g) (Figure 3). This result indicates that [^{18}F]**1** has desirable pharmacokinetics in normal mice, which is most likely due to a triazole substitution in place of a phenyl ring of stilbene that results in the reduction of both lipophilicity and nonspecific binding.

There are a few radiopharmaceuticals undergoing commercial development for PET imaging of Aβ plaques, including [^{18}F]GE-067, [^{18}F]BAY-94−9172, and [^{18}F]AV-45. [^{18}F]GE-067

dx.doi.org/10.1021/jm201400q | J. Med. Chem. 2012, 55, 883−892

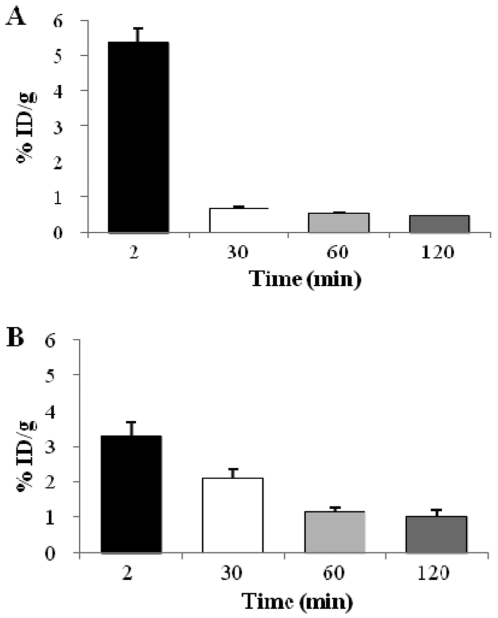

Figure 2. Brain uptake of [^{18}F]**1** (A) and [^{18}F]**5** (B) as a function of time in normal mice.

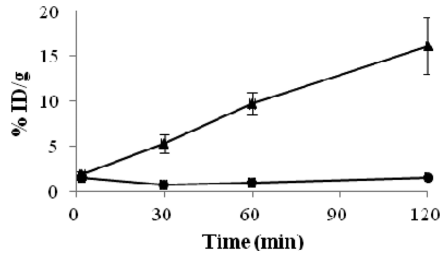

Figure 3. Femur uptake of [^{18}F]**1** (circle) and [^{18}F]**5** (triangle) as a function of time in normal mice.

had high binding affinity to AD brain homogenates (K_i = 0.74 nM; 5.9 nM to Aβ(1−40) aggregates) with high 2-to-30 min ratio of 8.4 in normal rodents.[36,50] [^{18}F]BAY94-9172 had high binding affinity to AD brain homogenates (K_i = 2.22 nM), suitable lipophilicity (log P = 2.41), and high initial brain uptake (7.77% ID/g) with fast wash-out (2-to-30 min ratio = 4.89) in normal mice.[33,34] [^{18}F]AV-45 also showed high binding affinity to AD brain homogenates (K_i = 2.87 nM), suitable lipophilicity (log P = 2.41), and high initial brain uptake (7.33% ID/g) with fast wash-out (2-to-60 min ratio = 3.90) in normal mice.[51] Compared with these radiopharmaceuticals, radioligand [^{18}F]**1** exhibited comparable pharmacokinetics, thus offering the promise as an Aβ plaque imaging radioligand.

In contrast, tissue distribution of [^{18}F]**5** showed high radioactivity accumulation in the heart (7.22% ID/g), lung (8.17% ID/g), liver (14.35% ID/g), and kidneys (10.46% ID/g) at 2 min postinjection, which decreased over time (Table 3). The brain uptake was 3.26% ID/g at 2 min postinjection and slowly washed out as a function of time (2.09% ID/g at 30 min and 1.13% ID/g at 60 min; 2-to-30 min ratio: 1.6, 2-to-60 min ratio: 2.9) (Figure 2B). Furthermore, increased femur uptake of [^{18}F]**5** with time indicated severe in vivo metabolic defluorination. This result suggests that [^{18}F]**5** may not be suitable for Aβ plaque imaging (Figure 3).

Table 3. Tissue Distribution of [^{18}F]5 in Normal Mice[a]

organ	2 min	30 min	60 min	120 min
blood	2.08 ± 0.15	0.98 ± 0.05	0.43 ± 0.05	0.38 ± 0.06
heart	7.22 ± 0.65	1.35 ± 0.35	0.56 ± 0.08	0.61 ± 0.06
lung	8.17 ± 0.97	1.72 ± 0.14	1.08 ± 0.07	1.16 ± 0.24
liver	14.35 ± 0.69	5.99 ± 1.09	2.47 ± 0.61	4.47 ± 1.43
spleen	3.15 ± 1.15	1.23 ± 0.17	0.84 ± 0.07	0.97 ± 0.64
kidney	10.46 ± 3.00	2.86 ± 1.36	2.76 ± 0.58	1.65 ± 0.19
muscle	3.67 ± 1.18	1.27 ± 0.15	0.74 ± 0.43	1.07 ± 0.50
femur	1.88 ± 0.26	5.24 ± 1.00	9.73 ± 1.23	16.15 ± 3.10
brain	3.26 ± 0.42	2.09 ± 0.25	1.13 ± 0.11	1.00 ± 0.19

[a]Values (% ID/g) are given as the means ± SD of groups, n = 4 mice.

CONCLUSIONS

A styryltriazole and four resveratrol derivatives were synthesized and evaluated in vitro and in vivo. Of the derivatives, [^{18}F]**5** showed the highest binding affinity to Aβ(1−42) aggregates; however, it showed slow pharmacokinetics in normal mouse brains with metabolic defluorination. In contrast, [^{18}F]**1** displayed good binding affinity to Aβ(1−42) aggregates and high initial uptake in and fast wash-out from normal mouse brains. These results suggest that [^{18}F]**1** is a potential radioligand for Aβ plaque imaging.

EXPERIMENTAL SECTION

Chemicals were purchased from Sigma-Aldrich (St. Louis, MO). Aβ(1−42) peptide was obtained from Bachem (Bubendorf, Switzerland), and Na^{125}I was from PerkinElmer (Waltham, MA). ^{1}H NMR spectra were obtained using a Varian ^{Unity}*Inova* 500NB (500 MHz) spectrometer (Palo Alto, CA) or a Bruker Avance 500 (500 MHz) spectrometer (Rheinstetten, Germany), and chemical shifts (δ) were reported as the ppm downfield of the internal tetramethylsilane. Electron impact (EI) and chemical ionization (CI) mass spectra were obtained using a JMS-700 Mstation (JEOL, Tokyo, Japan). For purification and analysis of radioligands, HPLC was conducted using the SpectraSYSTEM (Thermo Electron, Waltham, MA) equipped with a semipreparative column (YMC-Pack C18, 5 μ, 10 × 250 mm) or an analytical column (YMC-Pack C18, 5 μ, 4.6 × 250 mm). The eluent was monitored simultaneously, using UV (254 nm) and NaI(T1) radioactivity detectors. TLC was performed on Merck F_{254} silica plates and analyzed on a Bioscan radio-TLC scanner (Washington, DC).

[^{18}F]Fluoride was produced by the ^{18}O(p,n)^{18}F reaction using a GE Healthcare PETtrace cyclotron (Uppsala, Sweden). Radioactivity was measured in a dose calibrator (Biodex Medical Systems, Shirley, NY), and tissue radioactivity was measured in a Wizard^2 automatic gamma counter (PerkinElmer, Waltham, MA). All animal experiments were performed in compliance with the Laboratory Animal Care rules of the Samsung Medical Center.

Diethyl 4-Nitrobenzylphosphonate (6). A solution of 4-nitrobenzyl bromide (1.0 g, 4.62 mmol) in triethyl phosphite (801 μL, 4.66 mmol) was stirred at 160 °C for 3 h using a pressure vial. The reaction mixture was transferred to a round-bottomed flask using ethyl acetate and then concentrated in vacuo. Flash column chromatography (30:1 CH_2Cl_2-methanol) gave **6** (1.08 g, 85%) as a light-yellow oil. ^{1}H NMR ($CDCl_3$) δ 1.27 (t, J = 7.0 Hz, 6H), 3.24 (d, J = 22.5 Hz, 2H), 4.02−4.08 (m, 4H), 7.47 (d, J = 11.0 Hz, 2H), 8.18 (d, J = 8.0 Hz, 2H). MS (EI) m/z 273 (M^+). HRMS calcd for $C_{11}H_{16}NO_5P$, 273.0766; found, 273.0765.

(*E*)-1-(2-(Methoxymethoxy)ethyl)-4-(4-nitrostyryl)-1*H*-1,2,3-triazole (8). Potassium *t*-butoxide (134 mg, 1.19 mmol) was added to a solution of **6** (150 mg, 0.54 mmol) and **7** (100 mg, 0.54 mmol) in DMF (2.75 mL) at 0 °C. The reaction mixture was warmed to room temperature and stirred for 1 h. The mixture was then treated with water (50 mL) and extracted twice with ethyl acetate (50 mL); then, the combined organic layer was washed with water (150 mL) and

dx.doi.org/10.1021/jm201400q | J. Med. Chem. 2012, 55, 883−892

dried over Na_2SO_4. Flash column chromatography (1:2 hexane−ethyl acetate) afforded **8** (106 mg, 65%) as a yellow solid. mp 94−96 °C. ^{1}H NMR ($CDCl_3$) δ 3.29 (s, 6H), 3.95 (t, J = 5.0 Hz, 2H), 4.61 (t, J = 5.0 Hz, 2H), 4.62 (s, 2H), 7.24 (d, J = 17.5 Hz, 1H), 7.41 (d, J = 16.5 Hz, 1H), 7.62 (d, J = 5.0 Hz, 2H), 7.79 (s, 1H), 8.22 (d, J = 9.0 Hz, 2H). MS (EI) m/z 304 (M^+). HRMS calcd for $C_{14}H_{16}N_4O_4$, 304.1168; found, 304.1171.

(*E*)-4-(4-Aminostyryl)-1-(2-hydroxyethyl)-1*H*-1,2,3-triazole (9). $SnCl_2{\cdot}2H_2O$ (303 mg, 1.34 mmol) and conc. HCl (307 μL) were added to a solution of **8** (100 mg, 0.328 mm0l) in EtOH (6.2 mL), and the reaction mixture was stirred at 80 °C for 2 h. The mixture was neutralized with a saturated $NaHCO_3$ solution (aq, 50 mL) and extracted twice with ethyl acetate (200 mL), and then the combined organic layer was washed with brine (200 mL) and dried over Na_2SO_4. Compound **9** (50 mg, 76%) was obtained as a yellow solid. ^{1}H NMR (acetone-d_6) δ 3.99 (t, J = 5.0 Hz, 2H), 4.51 (t, J = 5.0 Hz, 2H), 6.90 (d, J = 16.5 Hz, 1H), 7.12 (d, J = 16.0 Hz, 1H), 7.30 (d, J = 6.0 Hz, 2H), 7.53 (d, J = 8.0 Hz, 2H), 8.05 (s, 1H). MS (EI) m/z 230 (M^+). HRMS calcd for $C_{12}H_{14}N_4O$, 230.1170; found, 230.1167.

(*E*)-1-(2-Hydroxyethyl)-4-(4-*N*,*N*-dimethylaminostyryl)-1*H*-1,2,3-triazole (10). Sodium cyanoborohydride (36.8 mg, 0.58 mmol) was added to a solution of **9** (45 mg, 0.19 mmol) and paraformaldehyde (58.6 mg, 1.95 mmol) in acetic acid (9 mL), which was allowed to stir at room temperature for 20 h. The reaction mixture was then neutralized with a saturated $NaHCO_3$ solution (aq, 250 mL) and extracted twice with ethyl acetate (200 mL); then, the combined organic layer was washed with water (200 mL) and dried over Na_2SO_4. Compound **10** (35 mg, 69%) was obtained as a yellow solid. ^{1}H NMR (CD_3OD) δ 2.97 (s, 6H), 3.96 (t, J = 5 Hz, 2H), 4.49 (t, J = 5 Hz, 2H), 6.76 (d, J = 9 Hz, 2H), 6.88 (d, J = 16.5 Hz, 1H), 7.19 (d, J = 16.5 Hz, 1H), 7.40 (d, J = 9 Hz, 2H), 8.02 (s, 1H). MS (EI) m/z 258 (M^+). HRMS calcd for $C_{14}H_{18}N_4O$, 258.1480; found, 258.1480.

(*E*)-1-(2-Methanesulfonyloxyethyl)-4-(4-*N*,*N*-dimethylaminostyryl)-1*H*-1,2,3-triazole (11). Triethylamine (161.9 μL, 1.16 mmol) was slowly added to a solution of **10** (50 mg, 0.193 mmol) in CH_2Cl_2 (1.5 mL), which was stirred at room temperature for 1 h. Methanesulfonyl chloride (30 μL, 0.387 mmol) was added to the solution at 0 °C, and the mixture was stirred at room temperature for 2 h. At the end of the reaction, the reaction mixture was diluted with water (50 mL) and extracted twice with ethyl acetate (50 mL); then, the combined organic layer was washed with brine (100 mL) and dried over Na_2SO_4. Flash column chromatography (1:3 hexane−ethyl acetate) afforded **11** (46 mg, 71%) as a light-yellow solid. mp 142−145 °C. ^{1}H NMR ($CDCl_3$) δ 2.95 (s, 6H), 2.99 (s, 3H), 4.70 (t, J = 5.0 Hz, 2H), 4.75 (t, J = 5.0 Hz, 2H), 6.69 (d, J = 9.0 Hz, 2H), 6.88 (d, J = 16.0 Hz, 1H), 7.40 (d, J = 8.5 Hz, 2H), 7.24 (d, J = 15.0 Hz, 1H), 8.10 (s, 1H). MS (EI) m/z 336 (M^+). HRMS calcd for $C_{15}H_{20}N_4O_3S$, 336.1256; found, 336.1260.

(*E*)-1-(2-Fluoroethyl)-4-(4-*N*,*N*-dimethylaminostyryl)-1*H*-1,2,3-triazole (1). Cesium fluoride (27 mg, 0.17 mmol) was added to a solution of **11** (20 mg, 0.06 mmol) in CH_3CN (1 mL), and the reaction mixture was stirred at 100 °C for 10 h. At the end of the reaction, the reaction mixture was diluted with water (20 mL) and extracted twice with ethyl acetate (30 mL), and the combined organic layer was then washed twice with water (20 mL) and dried over Na_2SO_4. Flash column chromatography (2:1 hexane−ethyl acetate) afforded **1** (7.2 mg, 47%) as a yellow solid. mp 126−127 °C. ^{1}H NMR ($CDCl_3$) δ 2.98 (s, 6H), 4.67 (dt, J = 27.0 and 4.5 Hz, 2H), 4.80 (dt, J = 47.0 and 4.5 Hz, 2H), 6.71 (d, J = 8.5 Hz, 2H), 6.89 (d, J = 16.5 Hz, 1H), 7.24 (d, J = 16.5 Hz, 1H), 7.39 (d, J = 9.0 Hz, 2H), 8.19 (s, 1H). MS (EI) m/z 260 (M^+). HRMS calcd for $C_{14}H_{17}FN_4$, 260.1437; found, 260.1440.

2-Azidoethanol (12). Sodium azide (3.146 g, 48.1 mmol) was added to a solution of 2-bromoethanol (2.26 mL, 32.1 mmol) in water (12 mL). The reaction mixture was stirred at 85 °C for 16 h.[52] At the end of the reaction, the mixture was diluted with water and extracted with diethyl ether (50 mL); then, the combined organic layer was washed with water (50 mL) and dried over Na_2SO_4. Compound **12** (1.97 g, 70%) was obtained as a colorless oil. ^{1}H NMR ($CDCl_3$) δ 3.47 (t, J = 5.0 Hz, 2H), 3.80 (t, J = 5.0 Hz, 2H); MS (CI) m/z 88 (M^+ + H). HRMS calcd for $C_2H_6N_3O$, 88.0511; found, 88.0513.

4-(Diethoxymethyl)-1-(2-hydroxyethyl)-1*H*-1,2,3-triazole (13). Sodium ascorbate (409 mg, 2.06 mmol) and $CuSO_4{\cdot}5H_2O$ (258 mg, 1.03 mmol) were added to a 1:1 *t*-butanol−water solution (19 mL) of 3,3-diethoxy-1-propyne (736 μL, 5.16 mmol) and **12** (450 mg, 5.16 mmol). The reaction mixture was stirred at room temperature for 4 h. At the end of the reaction, the mixture was diluted with water (100 mL) and extracted with CH_2Cl_2 (200 mL); then, the combined organic layer was washed with water (200 mL) and dried over Na_2SO_4. Flash column chromatography (15:1 CH_2Cl_2−methanol) afforded **13** (840 mg, 76%) as a colorless oil. ^{1}H NMR ($CDCl_3$) δ 1.24 (t, J = 7.0 Hz, 6H), 3.72 (q, J = 7.0 Hz, 4H), 4.11 (t, J = 5.0 Hz, 2H), 4.58 (t, J = 4.0 Hz, 2H), 8.26 (s, 1H), 10.15 (s, 1H). MS (CI) m/z 216 (M^+ + H). HRMS calcd for $C_9H_{18}N_3O_3$, 216.1348; found, 216.1346.

4-(Formyl)-1-(2-hydroxyethyl)-1*H*-1,2,3-triazole (14). Trifluoroacetic acid (4.4 mL, aq, 50%) was added dropwise to a solution of **13** (503 mg, 2.34 mmol) in $CHCl_3$ (13 mL) at 0 °C and stirred for 2 h at the same temperature. At the end of the reaction, the reaction mixture was concentrated in vacuo to remove $CHCl_3$ and neutralized with 1 N NaOH, extracted with ethyl acetate (100 mL); then, the combined organic layer was washed with brine (100 mL) and dried over Na_2SO_4. Compound **14** (300 mg, 91%) was obtained as a white solid. ^{1}H NMR ($CDCl_3$) δ 4.12 (t, J = 5.0 Hz, 2H), 4.59 (t, J = 5.0 Hz, 2H), 8.27 (s, 1H), 10.14 (s, 1H); MS (EI) m/z 141 (M^+). HRMS calcd for $C_5H_7N_3O_2$, 141.0538; found, 141.0539.

4-(Formyl)-1-(2-(methoxymethoxy)ethyl)-1*H*-1,2,3-triazole (7). DIPEA (741 μL, 4.25 mmol) was slowly added to a solution of **14** (300 mg, 2.12 mmol) in THF (15 mL) at 0 °C. Subsequently, chloromethylmethyl ether (323 μL, 4.251 mmol) was added dropwise at the same temperature. The resulting mixture was warmed to room temperature and stirred for 1 h and then at 65 °C for 16 h. At the end of the reaction, the mixture was quenched with a saturated NH_4Cl solution (aq, 100 mL) and extracted with ethyl acetate (100 mL). The combined organic layer was washed with brine (100 mL) and dried over Na_2SO_4. Flash column chromatography (30:1 CH_2Cl_2−methanol) gave **7** (230 mg, 58%) as a colorless oil. ^{1}H NMR ($CDCl_3$) δ 3.27 (s, 3H), 3.94 (t, J = 5.0 Hz, 2H), 4.61 (s, 2H), 4.64 (t, J = 5.0 Hz, 2H), 8.25 (s, 1H), 10.15 (s, 1H); MS (CI) m/z 186 (M^+ + H). HRMS calcd for $C_7H_{12}N_3O_3$, 186.0879; found, 186.0874.

Diethyl 3,5-Dimethoxybenzylphosphonate (15). A solution of 3,5-dimethoxybenzyl bromide (1.0 g, 4.32 mmol) in triethyl phosphite (750 μL, 4.37 mmol) was stirred at 160 °C for 4 h using a pressure vial. The reaction mixture was transferred to a round-bottomed flask using ethyl acetate (25 mL) and then concentrated in vacuo. Flash column chromatography (CH_2Cl_2-methanol 20:1) gave **15** (1.23 g, 99%) as a light-yellow oil. ^{1}H NMR ($CDCl_3$) δ 1.26 (t, J = 7.0 Hz, 6H), 3.07 (s, 1H), 3.11 (s, 1H), 3.78 (s, 6H), 4.02−4.05 (m, 4H), 6.35 (d, J = 2.0 Hz, 1H), 6.46 (t, J = 2.5 Hz, 2H). MS (EI) m/z 288 (M^+). HRMS calcd for $C_{13}H_{21}O_5P$, 288.1122; found, 288.1127.

(*E*)-1-(4-Fluorostyryl)-3,5-dimethoxybenzene (2). Potassium *t*-butoxide (233 mg, 2.08 mmol) was added to a solution of **15** (300 mg, 1.04 mmol) and 4-fluorobenzaldehyde (129 mg, 1.04 mmol) in DMF (5 mL) at 0 °C. The reaction mixture was warmed to room temperature and stirred for 1 h. At the end of the reaction, the mixture was diluted with water (30 mL) and extracted twice with ethyl acetate (50 mL); then, the combined organic layer was washed with brine (150 mL) and dried over Na_2SO_4. Flash column chromatography (10:1 hexane−ethyl acetate) afforded **2** (196 mg, 74%) as a white solid. mp 44−45 °C. ^{1}H NMR ($CDCl_3$) δ 3.83 (s, 6H), 6.40 (t, J = 2.0 Hz, 1H), 6.65 (d, J = 2.5 Hz, 2H), 6.94 (d, J = 16.0 Hz, 1H), 7.04 (d, J = 16.5 Hz, 1H), 7.05 (t, J = 11.0 Hz, 2H), 7.45−7.48 (m, 2H). MS (EI) m/z 258 (M^+). HRMS calcd for $C_{16}H_{15}O_2F$, 258.1075; found, 258.1056.

(*E*)-5-(4-Fluorostyryl)benzene-1,3-diol (3). BBr_3 (1 M) in CH_2Cl_2 (2.32 mL) was added dropwise to a solution of **2** (100 mg) in CH_2Cl_2 (1.6 mL) with vigorous stirring at 0 °C. The reaction mixture was warmed to room temperature and stirred for 20 h. After the addition of a saturated $NaHCO_3$ solution (aq, 20 mL), the mixture was extracted twice with CH_2Cl_2 (50 mL), and the combined organic layer was washed with water (50 mL) and dried over Na_2SO_4. Flash column

dx.doi.org/10.1021/jm201400q | J. Med. Chem. 2012, 55, 883−892

chromatography (20:1 CH_2Cl_2–methanol) afforded **3** (50 mg, 56%) as a white solid. mp 153–156 °C. ^{1}H NMR (CD_3OD) δ 6.21 (t, J = 2.0 Hz, 1H), 6.49 (d, J = 2.5 Hz, 2H), 6.94 (d, J = 16.0 Hz, 1H), 7.03 (d, J = 16.5 Hz, 1H), 7.07 (t, J = 8.5 Hz, 2H), 7.52–7.55 (m, 2H). MS (EI) m/z 302 (M^+). HRMS calcd for $C_{14}H_{11}O_2F$, 230.0745; found, 230.0743.

4-(2-Fluoroethoxy)benzaldehyde (16) and 4-(3-Fluoropropoxy)benzaldehyde (17). Fluoroalkyl tosylate (0.97 mmol) was added to a solution of 4-hydroxybenzaldehyde (100 mg, 0.82 mmol) and K_2CO_3 (212 mg, 0.98 mmol) in CH_3CN (17 mL), and the reaction mixture was stirred at 70 °C for 17 h. At the end of the reaction, the mixture was diluted with water and extracted with ethyl acetate (50 mL); then, the combined organic layer was washed with water (50 mL) and dried over Na_2SO_4. Flash column chromatography (hexane–ethyl acetate) afforded **16** (129 mg, 95%) or **17** (155 mg, 95%) as a white solid.

4-(2-Fluoroethoxy)benzaldehyde (16). ^{1}H NMR ($CDCl_3$) δ 4.31 (dt, J = 28.5 and 4.5 Hz, 2H), 4.79 (dt, J = 47.5 and 4 Hz, 2H), 7.04 (d, J = 9.0 Hz, 2H), 7.85 (d, J = 6.5 Hz, 2H), 9.90 (s, 1H). MS (EI) m/z 168 (M^+). HRMS calcd for $C_9H_9O_2F$, 168.0594; found, 168.0587.

4-(3-Fluoropropoxy)benzaldehyde (17). ^{1}H NMR ($CDCl_3$) δ 2.21 (dt, J = 26.0 and 6.0 Hz, 2H), 4.19 (t, J = 6.5 Hz, 2H), 4.66 (dt, J = 47.0 and 6.0 Hz, 2H), 7.01 (d, J = 7.0 Hz, 2H), 7.84 (d, J = 9.0 Hz, 2H), 9.89 (s, 1H). MS (EI) m/z 182 (M^+). HRMS calcd for $C_{10}H_{11}O_2F$, 182.0752; found, 182.0743.

(*E*)-1-(4-(2-Fluoroethoxy)styryl)-3,5-dimethoxybenzene (4) and (*E*)-1-(4-(3-Fluoropropoxy)styryl)-3,5-dimethoxybenzene (5). Potassium *t*-butoxide (133 mg, 1.18 mmol) was added to a solution of **15** (170 mg, 0.59 mmol) and **16** or **17** (0.59 mmol) in DMF (3 mL) at 0 °C. The reaction mixture was warmed to room temperature and stirred for 1 h. At the end of the reaction, the mixture was diluted with water and extracted twice with ethyl acetate (50 mL), and the resulting organic layer was washed with brine (150 mL) and dried over Na_2SO_4. Flash column chromatography (5:1 hexane–ethyl acetate) afforded **4** (100 mg, 56%) or **5** (118 mg, 63%) as a white solid.

(*E*)-1-(4-(2-Fluoroethoxy)styryl)-3,5-dimethoxybenzene (4). mp 82–83 °C. ^{1}H NMR ($CDCl_3$) δ 3.83 (s, 6H), 4.24 (dt, J = 28.0 and 4.0 Hz, 2H), 4.76 (dt, J = 47.5 and 4.0 Hz, 2H), 6.38 (t, J = 2.5 Hz, 1H), 6.64 (d, J = 2.5 Hz, 2H), 6.91 (d, J = 17.0 Hz, 1H), 6.91 (t, J = 8.5 Hz, 2H), 7.03 (d, J = 16.0 Hz, 1H), 7.45 (d, J = 4.5, 2H). MS (EI) m/z 302 (M^+). HRMS calcd for $C_{18}H_{19}O_3F$, 302.1308; found, 302.1318.

(*E*)-1-(4-(3-Fluoropropoxy)styryl)-3,5-dimethoxybenzene (5). mp 61–62 °C. ^{1}H NMR ($CDCl_3$) δ 2.18 (dt, J = 26.0 and 6.0 Hz, 2H), 3.82 (s, 6H), 4.12 (t, J = 6.0 Hz, 2H), 4.65 (dt, J = 47.0 and 6.0 Hz, 2H), 6.37 (t, J = 2.5 Hz, 1H), 6.64 (d, J = 2.5 Hz, 2H), 6.90 (d, J = 16.0 Hz, 1H), 6.90 (t, J = 8.0 Hz, 2H), 7.03 (d, J = 16.5 Hz, 1H), 7.43 (d, J = 8.5 Hz, 2H). MS (EI) m/z 316 (M^+). HRMS calcd for $C_{19}H_{21}O_3F$, 316.1467; found, 316.1475.

4-(Methoxymethoxy)benzaldehyde (18). DIPEA (2.56 mL, 14.73 mmol) was slowly added to a solution of 4-hydroxybenzaldehyde (900 mg, 7.37 mmol) in THF (30 mL) at 0 °C, with the subsequent dropwise addition of chloromethylmethyl ether (1.119 mL, 14.73 mmol) at the same temperature. The reaction mixture was warmed to room temperature and stirred for 1 h and then at 65 °C for 20 h. At the end of the reaction, the mixture was quenched with a saturated NH_4Cl solution (aq, 200 mL) and extracted with ethyl acetate (200 mL); then, the combined organic layer was washed with brine (200 mL) and dried over Na_2SO_4. Flash column chromatography (3:1 hexane–ethyl acetate) gave **18** (1.16 g, 95%) as a colorless oil. ^{1}H NMR ($CDCl_3$) δ 3.49 (s, 3H), 5.25 (s, 2H), 7.15 (d, J = 8.5 Hz, 2H), 7.84 (d, J = 9.0 Hz, 2H), 9.91 (s, 1H). MS (CI) m/z 167 (M^+). HRMS calcd for $C_9H_{11}O_3$, 167.0711; found, 167.0708.

(*E*)-1-(4-(Methoxymethoxy)styryl)-3,5-dimethoxybenzene (19). Potassium *t*-butoxide (311 mg, 2.77 mmol) was added to a solution of **15** (300 mg, 1.04 mmol) and **18** (173 mg, 1.04 mmol) in DMF (5.3 mL) at 0 °C. The reaction mixture was warmed to room temperature and stirred for 1 h. At the end of the reaction, the mixture was treated with water and extracted twice with ethyl acetate (200 mL); then, the combined organic layer was washed with water (200 mL) and dried over Na_2SO_4. Flash column chromatography (3:1 hexane–ethyl acetate) afforded **19** (176 mg, 56%) as a colorless oil. ^{1}H NMR ($CDCl_3$) δ 3.49 (s, 3H), 3.82 (s, 6H), 5.19 (s, 2H), 6.38 (t, J = 2.5 Hz, 1H), 6.65 (d, J = 2.0 Hz, 2H), 6.91 (d, J = 16.5 Hz, 1H), 7.02 (d, J = 8.5 Hz, 2H), 7.03 (d, J = 16.5 Hz, 1 H), 7.43 (d, J = 9.0 Hz, 2H). MS (EI) m/z 300 (M^+). HRMS calcd for $C_{18}H_{20}O_4$, 300.1361; found, 300.1361.

(*E*)-1-(4-Hydroxystyryl)-3,5-dimethoxybenzene (20). Five mL of 6 N HCl was added to a solution of **19** (560 mg, 1.864 mmol) in THF (10 mL) and was allowed to stir at room temperature for 1 h. At the end of the reaction, the reaction mixture was treated with water (100 mL) and extracted with ethyl acetate (200 mL); then, the combined organic layer was washed with water (200 mL) and dried over Na_2SO_4. Flash column chromatography (2:1 hexane–ethyl acetate) gave **20** (411 mg, 86%) as a white solid. ^{1}H NMR ($CDCl_3$) δ 3.82 (s, 6H), 6.37 (t, J = 2.5 Hz, 1H), 6.64 (d, J = 2.0 Hz, 2H), 6.82 (d, J = 7.0 Hz, 2H), 6.89 (d, J = 16.5 Hz, 1H), 7.02 (d, J = 16.5 Hz, 1 H), 7.39 (d, J = 7.0 Hz, 2H). MS (EI) m/z 256 (M^+). HRMS calcd for $C_{16}H_{16}O_3$, 256.1099; found, 256.1098.

(*E*)-1-(4-(3-Hydroxypropoxy)styryl)-3,5-dimethoxybenzene (21). 3-Chloropropanol (130 μL, 1.56 mmol) was added to a solution of K_2CO_3 (216 mg, 1.56 mmol) and **20** (200 mg, 0.78 mmol) in DMF (15 mL), and the reaction mixture was stirred at 160 °C for 20 h. At the end of the reaction, the reaction mixture was quenched with a saturated NH_4Cl solution (aq, 100 mL) and extracted with ethyl acetate (200 mL); then, the combined organic layer was washed with water (300 mL) and dried over Na_2SO_4. Flash column chromatography (3:1 hexane–ethyl acetate) afforded **21** (190 mg, 78%) as a white solid. mp 92–93 °C. ^{1}H NMR ($CDCl_3$) δ 2.03–2.08 (m, 2H), 3.82 (s, 6H), 3.87 (t, J = 6.0 Hz, 2H), 4.15 (t, J = 6.0 Hz, 2H), 6.37 (t, J = 2.5 Hz, 1H), 6.64 (d, J = 2.0 Hz, 2H), 6.88–6.91 (m, 3H), 7.03 (d, J = 16.5 Hz, 1H), 7.43 (d, J = 9.0 Hz, 2H). MS (EI) m/z 314 (M^+). HRMS calcd for $C_{19}H_{22}O_4$, 314.1518; found, 314.1514.

(*E*)-1-(4-(3-Toluenesulfonylpropoxy)styryl)-3,5-dimethoxybenzene (22). Triethylamine (319 μL, 2.29 mmol) was slowly added to a solution of **21** (120 mg, 0.38 mmol) in CH_2Cl_2 (3 mL), and the reaction mixture was stirred at room temperature for 1 h. *p*-Toluenesulfonyl chloride (145 mg, 0.76 mmol) was added to the solution, which was allowed to stir at room temperature for 2 h. At the end of the reaction, the mixture was treated with water (50 mL) and extracted twice with CH_2Cl_2 (50 mL); then, the combined organic layer was washed with brine (100 mL) and dried over Na_2SO_4. Flash column chromatography (3:1 hexane–ethyl acetate) gave **22** (100 mg, 56%) as a white solid. mp 102–103 °C. ^{1}H NMR ($CDCl_3$) δ 2.09–2.14 (m, 2H), 2.37 (s, 3H), 3.83 (s, 6H), 3.96 (t, J = 6.0 Hz, 2H), 4.25 (t, J = 6.0 Hz, 2H), 6.38 (t, J = 2.5 Hz, 1H), 7.65 (d, J = 2.0 Hz, 2H), 7.74 (d, J = 11.0 Hz, 2H), 6.89 (d, J = 16.0 Hz, 1H), 7.03 (d, J = 16.5 Hz, 1H), 7.24 (d, J = 7.5 Hz, 2H), 7.40 (d, J = 8.5 Hz, 2H), 7.75 (d, J = 8.0 Hz, 2H). MS (EI) m/z 468 (M^+). HRMS calcd for $C_{26}H_{28}O_6S$, 468.1606; found, 468.1610.

(*E*)-1-(2-[^{18}F]Fluoroethyl)-4-(4-*N*,*N*-dimethylaminostyryl)-1*H*-1,2,3-triazole ([^{18}F]1) and (*E*)-1-(4-(3-[^{18}F]Fluoropropoxy)-styryl)-3,5-dimethoxybenzene ([^{18}F]5). [^{18}F]Fluoride (740–925 MBq) was placed in a Vacutainer containing *n*-Bu_4NHCO_3. Three azeotropic distillations were then performed using 100–200 μL aliquots of CH_3CN at 90 °C (oil bath) under a gentle stream of N_2. The resulting *n*-Bu_4N[^{18}F]F was then dissolved in CH_3CN (200 μL) and transferred to a reaction vial containing the precursor **11** (2 mg, 5.94 μmol) or **22** (2 mg, 4.25 μmol). The reaction mixture was stirred at 90 or 110 °C for 10 min ([^{18}F]**1** or [^{18}F]**5**, respectively). At the end of the reaction, the mixture was cooled, treated with water (2 mL), and extracted with ethyl acetate (2 mL). The organic layer was washed with water and passed through a 2 cm Na_2SO_4 plug, and the solvent was removed under a stream of N_2 at 50 °C (water bath). The crude product was then purified by HPLC using a semipreparative column eluted with a 60:40 mixture of 10 mM ammonium formate (aq) and acetonitrile at a flow rate of 4.0 mL/min for [^{18}F]**1** or a 40:60 mixture of 0.1% TFA in water and acetonitrile for [^{18}F]**5**. The desired products eluted between 18 and 19 min for [^{18}F]**1** and between 29 and 30 min

dx.doi.org/10.1021/jm201400q | *J. Med. Chem.* 2012, 55, 883–892

for [^{18}F]**5**. The radioligand was concentrated under a gentle stream of N_2, redissolved in ethanol, and diluted with saline to give a final solution of 10% ethanol in saline.

Specific activity was determined by comparing UV peak area of the desired radioactive peak and the UV peak areas of different concentrations of unlabeled standard **1** or **5** on HPLC. Identity of radioligand [^{18}F]**1** or [^{18}F]**5** was determined by coinjecting the radioligand with the corresponding unlabeled standard into the HPLC system.

In Vitro Binding Assays Using Aβ(1−42) Aggregates. Aβ(1−42) peptide (0.25 mg) was dissolved in sodium phosphate buffer (10 mM, 1 mL) containing 1 mM EDTA (pH 7.4) and stirred gently at 37 °C for 42 h. Binding studies were conducted using a previously described method.[15] For saturation binding studies, Aβ(1−42) aggregates were added to mixtures containing [^{125}I]TZDM (50 μL, 0.01−8 nM in 40% ethanol). The final concentration of ethanol in a total volume of 1 mL of solution was 10%. Nonspecific binding was determined in the presence of 10 μM thioflavin-T (50 μL in 40% ethanol). For inhibition studies, a total volume of 1 mL containing the ligand **1**−**5** or TZDM (50 μL, 10^{-5} to 10^{-10} M in 40% ethanol) and 0.1 nM of [^{125}I]TZDM (50 μL in 40% EtOH) was used. Reaction mixtures were incubated with shaking at room temperature for 3 h, and the bound radioactivity was collected on Whatman GF/B filters using a cell harvester and washed twice using 3 mL of 10% ethanol. The filters containing radioactivity were then counted using a gamma counter. Data were analyzed using GraphPad Prism software, and the K_d and K_i values were calculated.

Partition Coefficient Measurement. The radioligand ([^{18}F]**1** or [^{18}F]**5**) was added to a premixed suspension containing 600 μL of octanol and 600 μL of water, vortexed vigorously for 3 min, and then centrifuged. Two layers were separated, and 100 μL aliquots of the octanol and aqueous layers were removed and counted. Samples from the octanol and aqueous layers repartitioned until consistent values were obtained. The experiments were conducted in triplicate. The log *P* is expressed as the logarithm of the ratio of the counts per minute of octanol versus that of water.

Tissue Distribution in Normal Mice. ICR mice (male, 25−30 g, four mice per time point) were injected with [^{18}F]**1** or [^{18}F]**5** (1.11 MBq) in 0.2 mL of 10% ethanol-saline via a tail vein and sacrificed at the indicated time points (2, 30, 60, and 120 min). Samples of blood, heart, lung, liver, spleen, kidney, muscle, femur, and brain were removed, weighed, and counted. Data are expressed as the percent injected dose per gram of tissues (% ID/g).

■ ASSOCIATED CONTENT

Ⓢ Supporting Information

^{1}H NMR spectra and HRMS data of precursors (**11** and **22**) and target ligands (**1** and **5**); HPLC chromatograms of precursors, target ligands, and final radioliogands ([^{18}F]**1** and [^{18}F]**5**). This material is available free of charge via the Internet at http://pubs.acs.org.

■ AUTHOR INFORMATION

Corresponding Author

*Tel: +82-2-3410-2623. Fax: +82-2-3410-2667. E-mail: ysnm.choe@samsung.com.

■ ACKNOWLEDGMENTS

This study was partially supported by a Nuclear Research Development Program of the Korea Science and Engineering Foundation (KOSEF) grant funded by the Korean government (MEST) (grant code: 2010-0018315).

■ ABBREVIATIONS USED

Aβ, β-amyloid; PET, positron emission tomography; AD, Alzheimer's disease; NFTs, neurofibrillary tangles; HPLC, high-performance liquid chromatography; TLC, thin layer chromatography; MOM, methoxymethyl

■ REFERENCES

(1) Ginsberg, S. D.; Schmidt, M. L.; Crino, P. B.; Eberwine, J. H.; Lee, V. M. Y.; Trojanowski, J. Q. Molecular Pathology of Alzheimer's Disease and Related Disorders. In *Cerebral Cortex: Neurodegenerative and Age-Related Changes in Structure and Function of Cerebral Cortex*; Kluwer Academic/Plenum: New York, 1999; pp 603−654.

(2) Lee, V. M.; Trojanowski, J. Q. Neurodegenerative Tauopathies: Human Disease and Transgenic Mouse Models. *Neuron* **1999**, *24*, 507−510.

(3) Selkoe, D. J. The Origins of Alzheimer Disease: A is for Amyloid. *JAMA, J. Am. Med. Assoc.* **2000**, *283*, 1615−1617.

(4) Mathis, C. A.; Wang, Y.; Klunk, W. E. Imaging β-Amyloid Plaques and Neurofibrillary Tangles in the Aging Human Brain. *Curr. Pharm. Design* **2004**, *10*, 1469−1492.

(5) Agdeppa, E. D.; Kepe, V.; Liu, J.; Flores-Torres, S.; Satyamurthy, N.; Petric, A.; Cole, G. M.; Small, G. W.; Huang, S. C.; Barrio, J. R. Binding Characteristics of Radiofluorinated 6-Dialkylamino-2-Naphthalylethylidene Derivatives as Positron Emission Tomography Imaging Probes of ß-Amyloid Plaques in Alzheimer's Disease. *J. Neurosci.* **2001**, *21*, RC189.

(6) Barrio, J. R.; Huang, S. C.; Cole, G.; Satyamurthy, N.; Petric, A.; Phelps, M. E.; Small, G. PET Imaging of Tangles and Plaques in Alzheimer Disease with a Highly Hydrophobic Probe. *J. Labelled. Compd. Radiopharm.* **1999**, *42*, S194−195.

(7) Kung, H. F.; Lee, C. W.; Zhuang, Z. P.; Kung, M. P.; Hou, C.; Plössl, K. Novel Stilbenes as Probes for Amyloid Plaques. *J. Am. Chem. Soc.* **2001**, *123*, 12740−12741.

(8) Mathis, C. A.; Bacskai, B. J.; Kajdasz, S. T.; McLellan, M. E.; Frosch, M. P.; Hyman, B. T.; Holt, D. P.; Wang, Y.; Huang, G.-F.; Debnath, M. L.; Klunk, W. E. A Lipophilic Thioflavin-T Derivative for Positron Emission Tomography (PET) Imaging of Amyloid in Brain. *Bioorg. Med. Chem. Lett.* **2002**, *12*, 295−298.

(9) Mathis, C. A.; Wang, Y.; Holt, D. P.; Huang, G. F.; Debnath, M. L.; Klunk, W. E. Synthesis and Evaluation of ^{11}C-Labeled 6-Substituted 2-Arylbenzothiazoles as Amyloid Imaging Agents. *J. Med. Chem.* **2003**, *46*, 2740−2754.

(10) Klunk, W. E.; Engler, H.; Nordberg, A.; Wang, Y.; Blomqvist, G.; Holt, D. P.; Bergström, M.; Savitcheva, I.; Huang, G.; Estrada, S.; Ausén, B.; Debnath, M. L.; Barletta, J.; Price, J. C.; Sandell, J.; Lopresti, B. J.; Wall, A.; Koivisto, P.; Antoni, G.; Mathis, C. A.; Långström, B. Imaging Brain Amyloid in Alzheimer's Disease with Pittsburgh Compound-B. *Ann. Neurol.* **2004**, *55*, 306−319.

(11) Lopresti, B. J.; Klunk, W. E.; Mathis, C. A.; Hoge, J. A.; Ziolko, S. K.; Lu, X.; Meltzer, C. C.; Schimmel, K.; Tsopelas, N. D.; DeKosky, S. T.; Price, J. C. Simplified Quantification of Pittsburgh Compound B Amyloid Imaging PET Studies: A Comparative Analysis. *J. Nucl. Med.* **2005**, *46*, 1959−1972.

(12) Rowe, C. C.; Ng, S.; Ackermann, U.; Gong, S. J.; Pike, K.; Savage, G.; Cowie, T. F.; Dickinson, K. L.; Maruff, P.; Darby, D.; Smith, C.; Woodward, M.; Merory, J.; Tochon-Danguy, H.; O'Keefe, G.; Klunk, W. E.; Mathis, C. A.; Price, J. C.; Masters, C. L.; Villemage, V. L. Imaging β-Amyloid Burden in Aging and Dementia. *Neurology* **2007**, *68*, 1718−1725.

(13) Johnson, A. E.; Jeppsson, F.; Sandell, J.; Wensbo, D.; Neelissen, J. A. M.; Juréus, A.; Ström, P.; Norman, H.; Farde, L.; Svensson, S. P. S. AZD2184: a Radioligand for Sensitive Detection of β-Amyloid Deposits. *J. Neurochem.* **2009**, *108*, 1177−1186.

(14) Yousefi, B. H.; Manook, A.; Drzezga, A.; Reutern, B. V.; Schwaiger, M.; Wester, H.-J.; Henriksen, G. Synthesis and Evaluation of ^{11}C-Labeled Imidazo[2,1-*b*]benzothiazoles (IBTs) as PET Tracers for Imaging β-Amyloid Plaques in Alzheimer's Disease. *J. Med. Chem.* **2011**, *54*, 949−956.

(15) Ono, M.; Wilson, A.; Nobrega, J.; Westaway, D.; Verhoeff, P.; Zhuang, Z. P.; Kung, M. P.; Kung, H. F. ^{11}C-Labeled Stilbene Derivatives as Aß-Aggregate-Specific PET Imaging Agents for Alzheimer's Disease. *Nucl. Med. Biol.* **2003**, *30*, 565−571.

(16) Zhuang, Z. P.; Kung, M. P.; Hou, C.; Skovronsky, D. M.; Gur, T. L.; Trojanowski, J. Q.; Lee, V. M. Y.; Kung, H. F. Radioiodinated

Styrylbenzenes and Thioflavins as Probes for Amyloid Aggregates. *J. Med. Chem.* **2001**, *44*, 1905−1914.
(17) Zhuang, Z. -P.; Kung, M. P.; Hou, C.; Plössl, K.; Skovronsky, D.; Gur, T. L.; Trojanowski, J. Q.; Lee, V. M. Y.; Kung, H. F. IBOX (2-(4′-dimethylaminophenyl)-6-iodobenzoxazole): A Ligand for Imaging Amyloid Plaques in the Brain. *Nucl. Med. Biol.* **2001**, *28*, 887−894.
(18) Zhuang, Z. P.; Kung, M. P.; Wilson, A.; Lee, C. H.; Plössl, K.; Hou, C.; Holtzman, D. M.; Kung, H. F. Structure-Activity Relationship of Imidazo[1,2-a]pyridines as Ligands for Detecting ß-Amyloid Plaques in the Brain. *J. Med. Chem.* **2003**, *46*, 237−243.
(19) Kung, M. P.; Hou, C. H.; Zhuang, Z. P.; Cross, A. J.; Maier, D. L.; Kung, H. F. Characterization of IMPY as a Potential Imaging Agent for *β*-Amyloid Plaques in Double Transgenic PSAPP Mice. *Eur. J. Nucl. Med. Mol. Imaging* **2004**, *31*, 1136−1145.
(20) Kung, M. P.; Hou, C. H.; Zhuang, Z. P.; Skovronsky, D.; Kung, H. F. Binding of Two Potential Imaging Agents Targeting Amyloid Plaques in Postmortem Brain Tissues of Patients with Alzheimer's Disease. *Brain Res.* **2004**, *1025*, 98−105.
(21) Newberg, A. B.; Wintering, N. A.; Plossl, K.; Hochold, J.; Stabin, M. G.; Watson, M.; Skovronsky, D.; Clark, C. M.; Kung, M. P.; Kung, H. F. Safety, Biodistribution, and Dosimetry of ^{123}I-IMPY: a Novel Amyloid Plaque-Imaging Agent for the Diagnosis of Alzheimer's Disease. *J. Nucl. Med.* **2006**, *47*, 748−754.
(22) Chandra, R.; Oya, S.; Kung, M. P.; Hou, C.; Jin, L. W.; Kung, H. F. New Diphenylacetylenes as Probes for Positron Emission Tomographic Imaging of Amyloid Plaques. *J. Med. Chem.* **2007**, *50*, 2415−2423.
(23) Pagliai, F.; Pirali, T.; Del Grosso, E.; Di Brisco, R.; Tron, G. C.; Sorba, G.; Genazzani, A. A. Rapid Synthesis of Triazole-Modified Resveratrol Analogues via Click Chemistry. *J. Med. Chem.* **2006**, *49*, 467−470.
(24) Kolb, H. C.; Finn, M. G.; Sharpless, K. B. Click Chemistry: Diverse Chemical Function from a Few Good Reactions. *Angew. Chem., Int. Ed.* **2001**, *40*, 2004−2021.
(25) Kolb, H. C.; Sharpless, K. B. The Growing Impact of Click Chemistry on Drug Discovery. *Drug Discovery Today* **2003**, *8*, 1128−1137.
(26) Sharpless, K. B.; Manetsch, R. In Situ Click Chemistry: a Powerful Means for Lead Discovery. *Expert Opin. Drug Discovery* **2006**, *1*, 525−538.
(27) Qu, W.; Kung, M.-P.; Hou, C; Oya, S.; Kung, H. F. Quick Assembly of 1,4-Diphenyltriazoles as Probes Targeting *β*-Amyloid Aggregates in Alzheimer's Disease. *J. Med. Chem.* **2007**, *50*, 3380−3387.
(28) Juréus, A.; Swahn, B. M.; Sandell, J.; Jeppsson, F.; Johnson, A. E.; Johnström, P.; Neelissen, J. A. M.; Sunnemark, D.; Farde, L.; Svensson, S. P. S. Characterization of AZD4694, a Novel Fluorinated A*β* Plaque Neuroimaging PET Radioligand. *J. Neurochem.* **2010**, *114*, 784−794.
(29) Schou, M.; Johnström, P.; Varnäs, K.; Juréus, A.; Sandell, J.; Cselenyi, Z.; Swahn, B. M.; Svensson, S.; Lindström-Bööö, E.; Farde, L.; Halldin, C. [^{18}F]AZD4694 - A New ^{18}F-Labeled *β*-Amyloid Probe with Rapid Brain Washout. *J. Label. Compd. Radiopharm.* **2011**, *54*, S41.
(30) Yousefi, B. H.; Drzezga, A.; Reutern, B. v.; Manook, A.; Schwaiger, M.; Wester, H.-J.; Henriksen, G. A Novel ^{18}F-Labeled Imidazo[2,1-*b*]benzothiazole (IBT) for High-Contrast PET Imaging of *β*-Amyloid Plaques. *ACS Med. Chem. Lett.* **2011**, *2*, 673−677.
(31) Koole, M.; Lewis, D. M.; Buckley, C.; Nelissen, N.; Vandenbulcke, M.; Brooks, D. J.; Bandenbeghe, R.; Van Laere, K. Whole-Body Biodistribution and Radiation Dosimetry of ^{18}F-GE067: A Radioligand for In Vivo Brain Amyloid Imaging. *J. Nucl. Med.* **2009**, *50*, 818−822.
(32) Nelissen, N.; Laere, K. V.; Thurfjell, L.; Owenius, R.; Vandenbulcke, M.; Koole, M.; Bormans, G.; Brooks, D. J.; Vandenberghe, R. Phase 1 Study of the Pittsburgh Compound B Derivative ^{18}F-Flutemetamol in Healthy Volunteers and Patients with Probable Alzheimer Disease. *J. Nucl. Med.* **2009**, *50*, 1251−1259.
(33) Zhang, W.; Oya, S.; Kung, M. P.; Hou, C.; Marier, D. L.; Kung, H. F. F-18 Polyethylene Glycol Stilbenes as PET Imaging Agents Targeting A*β* Aggregates in the Brain. *Nucl. Med. Biol.* **2005**, *32*, 799−809.
(34) Rowe, C. C.; Ackerman, U.; Browne, W.; Mulligan, R.; Pike, K. L.; O'Keefe, G.; Tochon-Danguy, H.; Chan, G.; Berlangieri, S. U.; Jones, G.; Dickinson-Rowe, K. L.; Kung, H. F.; Zhang, W.; Kung, M. P.; Skovronsky, D.; Dyrks, T.; Holl, G.; Krause, S.; Friebe, M.; Lehman, L.; Lindemann, S.; Dinkelborg, L. M.; Masters, C. L.; Villemagne, V. L. Imaging of Amyloid beta in Alzheimer's Disease with ^{18}F-BAY94-9172, a Novel PET Tracer: Proof of Mechanism. *Lancet Neurol.* **2008**, *7*, 129−135.
(35) Zhang, W.; Kung, M. P.; Oya, S.; Hou, C.; Kung, H. F. ^{18}F-Labeld Styrylpyridines as PET Agents for Amyloid Plaque Imaging. *Nucl. Med. Biol.* **2007**, *34*, 89−97.
(36) Kung, H. F.; Choi, S. R.; Qu, W.; Zhang, W.; Skovronsky, D. ^{18}F Stilbenes and Styrylpyridines for PET Imaging of A*β* Plaques in Alzheimer's Disease: a Miniperspective. *J. Med. Chem.* **2010**, *53*, 933−941.
(37) Bastianetto, S.; Zheng, W.-H.; Quirion, R. Neuroprotective Abilities of Resveratrol and Other Red Wine Constituents Against Nitric Oxide-related Toxicity in Cultured Hippocampal Neuron. *Br. J. Pharmacol.* **2000**, *131*, 711−720.
(38) Hsieh, T.-C.; Juan, G.; Darzynkiewicz, Z.; Wu, J. M. Resveratrol Increases Nitric Oxide Synthase, Induces Accumulation of p53 and p21WAF1/CIP1, and Suppresses Cultured Bovine Pulmonary Artery Endothelial Cell Proliferation by Perturbing Progression Through S and G2. *Cancer Res.* **1999**, *59*, 2596−2601.
(39) Luchsinger, J. A.; Tang, M. X.; Siddique, M.; Shea, S.; Mayeux, R. Alcohol Intake and Risk of Dementia. *J. Am. Geriatr. Soc.* **2004**, *52*, 540−546.
(40) Marambaud, P.; Zhao, H.; Davies, P. Resveratrol Promotes Clearance of Alzheimer's Disease Amyloid-*β* Peptides. *J. Biol. Chem.* **2005**, *280*, 37377−37382.
(41) Feng, Y.; Wang, X. P.; Yang, S. G.; Wang, Y. J.; Zhang, X.; Du, X. T.; Sun, X. X.; Zhao, M.; Huang, L.; Liu, R. T. Resveratrol Inhibits *β*-Amyloid Oligomeric Cytotoxicity but Does Not Prevent Oligomer Formation. *Neurotoxicology* **2009**, *30*, 986−995.
(42) Gester, S.; Wuest, F.; Pawelke, B.; Bergmann, R.; Pietzsch, J. Synthesis and Biodistribution of an ^{18}F-Labelled Resveratrol Derivative for Small Animal Positron Emission Tomography. *Amino Acids* **2005**, *29*, 415−428.
(43) Yu, J.; Gaunt, M. J.; Spencer, J. B. Convenient Preparation of *trans*-Arylalkenes via Palladium(II)-Catalyzed Isomerization of cis-Arylalkenes. *J. Org. Chem.* **2002**, *67*, 4627−4629.
(44) Yin, J.; Zarkowsky, D. S.; Thomas, D. W.; Zhao, M. M.; Huffman, M. A. Direct and Convenient Conversion of Alcohols to Fluorides. *Org. Lett.* **2007**, *6*, 1465−1468.
(45) Wadsworth, W. S.; Emmons, W. D. The Utility of Phosphonate Carbanions in Olefin Synthesis. *J. Am. Chem. Soc.* **1961**, *83*, 1733−1738.
(46) Wadsworth, W. S.; Emmons, W. D. Ethyl Cyclohexylideneacetate. *Org. Synthesis* **1973**, *7*, 44.
(47) Chang, C. S.; Lin, Y. T.; Shih, S. R.; Lee, C. C.; Lee, Y. C.; Tai, C. L.; Tseng, S. N.; Chern, J. H. Design, Synthesis, and Antipicornavirus Activity of 1-[5-(4-Arylphenoxy)alkyl]-3-pyridin-4ylimidazolidin-2-one Derivatives. *J. Med. Chem.* **2005**, *48*, 3522−3535.
(48) Griec, P. A.; Nishizawa, M.; Oguru, T.; Burke, S. D.; Marinovic, N. (±)-Vernolepin and (±)-Vernomenin. *J. Am. Soc. Chem.* **1977**, *99*, 5773−5780.
(49) Mark, D. H.; Alberto, A. L.; Fred, A. M. Synthesis of 1-Bromoestradiol. *J. Org. Chem.* **1984**, *49*, 2744−2745.
(50) Mason, N.; Klunk, W.; Debnath, M.; Flatt, N.; Huang, G.; Shao, L.; Mathis, C. A. Synthesis of Evaluation of Aromatic Fluorinated [F-18]PIB Analogs as Abeta Plaque PET Imaging Agents. *J. Labelled Compd. Radiopharm.* **2009**, *52* (Suppl 1), S90.
(51) Choi, S. R.; Golding, G.; Zhuang, Z.; Zhang, W.; Lim, N; Hefti, F.; Benedum, T. E.; Kilbourn, M. R.; Skovronsky, D.; Kung, H. F.

Preclinical Properties of ^{18}F-AV-45: A PET Agent for Aβ Plaques in the Brain. *J. Nucl. Med.* **2009**, *50*, 1887−1894.
(52) Hooper, N.; Beeching, L. J.; Dyke, J. M.; Morris, A.; Ogden, J. S. A Study of the Thermal Decomposition of 2-Azidoethanol and 2-Azidoethyl Acetate by Ultraviolet Photoelectron Spectroscopy and Matrix Isolation Infrared Spectroscopy. *J. Phys. Chem. A* **2002**, *106*, 9968−9975.